Talanta 188 (2018) 27–34

Contents lists available at ScienceDirect

Talanta

journal homepage: www.elsevier.com/locate/talanta

Single polydiacetylene microtube waveguide platform for discriminating microRNA-215 expression levels in clinical gastric cancerous, paracancerous and normal tissues

Mengqiao Wang[a,1], Yue Yu[b,1], Funing Liu[a], Le Ren[b], Qijin Zhang[a], Gang Zou[a,*]

[a] CAS Key Laboratory of Soft Matter Chemistry, Department of Polymer Science and Engineering, iChEM, University of Science and Technology of China, Hefei, Anhui 230026, PR China

[b] Division of Gastroenterology, Affiliated Provincial Hospital, Anhui Medical University, No.17 Lu Jiang Road, Hefei, Anhui 230001, PR China

ARTICLE INFO

Keywords:
PDA microtube waveguide platform
Sandwich-type hybridization
Condensing enrichment effect
MicroRNA-215 detection
Clinical gastric cancerous tissues

ABSTRACT

MicroRNAs (miRNAs) have emerged as novel biomarkers for human early-phase cancer diagnosis and disease prevention recently. Herein, we reported a novel miRNA-215 targeting biosensor, which was based on single polydiacetylene (PDA) microtube waveguide system integrated with sandwich-type hybridization design and condensing enrichment effect. The target miRNA could be captured by oligonucleotides conjugated on the surface of PDA microtube and Au nanorod (AuNR) respectively, resulting in the out-coupled fluorescence of PDA microtube quenching. In this strategy, the formation of a sandwich structure, as a result of co-hybridization of the target miRNA, enabled simplified preparation process, enhanced reaction efficiency, and increased recyclability and stability of the platform. Based on condensing enrichment effect, the co-hybridization reaction could be enriched on the surface of microtube and the proposed platform could easily achieve highly sensitive detection of miRNA-215 in one step. Remarkably, this platform could be directly applied to discriminate the miRNA-215 expression levels in clinical gastric cancerous, paracancerous and normal tissues samples. This assay offers a simple and convenient method for miRNA quantification in clinical samples, even with the potential for invasive, portable equipment for early clinical diagnosis of diseases.

1. Introduction

In recent years, microRNAs (miRNAs) quantification techniques have attracted enormous attention [1–4] since the variation of miRNAs expression was found to be directly related to many diseases [5–8]. And miRNAs have emerged as new diagnostic and prognostic biomarkers for infection prevention, disease detection, and early-phase cancer diagnosis [9–11]. Extensive studies in this field are mainly focused on developing novel miRNAs quantification techniques, including quantitative reverse transcription polymerase chain reaction (qRT- PCR) [12–14], electrochemical methods [15,16], northern blotting [17,18], microarray hybridization [19,20], and so on. However, their further applications in clinical diagnosis are limited by some intrinsic drawbacks, including expensive instruments, low detection sensitivity, susceptible to interference from biological environment, time-consuming, tedious operation processes, and requirement for skilled operators. Fluorescence based methods have been widely used in miRNA detection due to their high sensitivity and easy operation [21–23]. Nevertheless, the traditional fluorescence methods possess some inevitable defects, including low stability and spectra cross-talk with background fluorescence in complex biology environment such as human serum. [24–26]. To address these issues, our group previously designed and constructed one dimensional (1D) AuNR-functionalized PDA microtube waveguide system for miRNA-21 detection, in which the emission excitation and out-coupled positions were far apart, reducing the background fluorescence interference [27]. However, due to strong adhesion of Au nanorods on the surface of PDA microtube, the efficiency of toehold strand displacement reaction within the surface of PDA microtube can be substantially reduced after long-term storage (e.g. one week), preventing its practical applications. Therefore, it remains challenging to develop novel structural design for target miRNA detection to improve stability and recyclability of the PDA microtube waveguide platform.

Owing to the merits of high reaction efficiency and simple preparation steps, sandwich-structural designs have been widely used in biosensing and biomedical field [28–30]. When the target presents, the

* Corresponding author.
E-mail address: gangzou@ustc.edu.cn (G. Zou).
[1] These authors contributed equally to this work.

https://doi.org/10.1016/j.talanta.2018.05.049
Received 28 December 2017; Received in revised form 18 March 2018; Accepted 13 May 2018
Available online 17 May 2018
0039-9140/ © 2018 Elsevier B.V. All rights reserved.

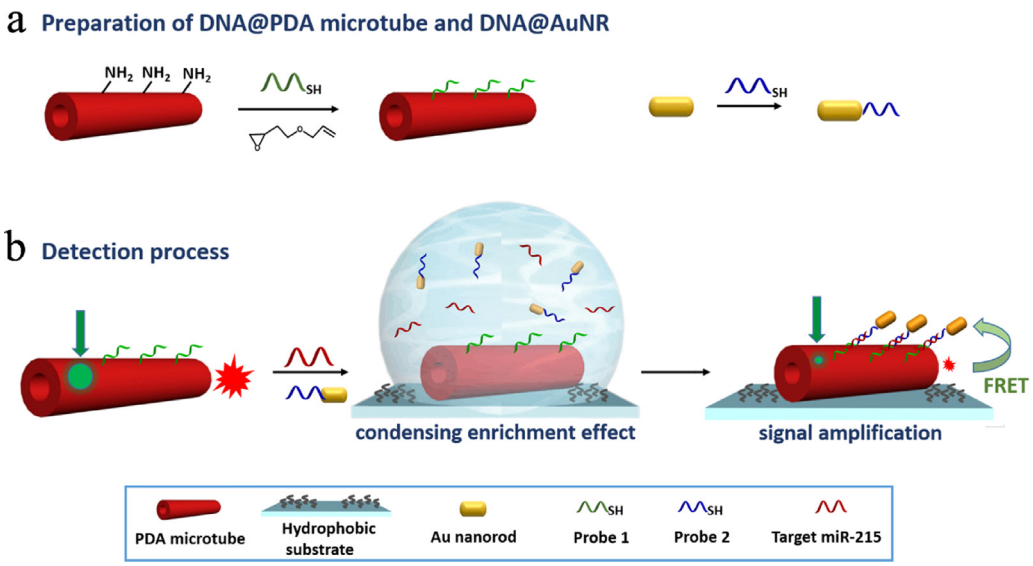

Scheme 1. (a) Preparation of Probe 1 modified PDA microtube and Probe 2 modified Au nanorods. (b) Schematic illustration for miRNA-215 detection strategies by sandwich type PDA biosensor integrated with condensing enrichment effect.

target analyte is sandwiched between capture probe (immobilized on the test zone of the assay) and detection probe (conjugated with nanoparticle). For instance, Zhang et al. reported a sensitive enzyme-amplified sandwich structure biosensor for visual detection of miRNA-224 with low limit of detection (LOD) (7.5 pM) [31]. Niazi et al. developed a capacitive aptamer–antibody based sandwich assay for sensitive detection of vascular endothelial growth factor-165 (VEGF), exhibiting enhanced signal with a highly sensitive detection of VEGF protein in human serum [32]. Nevertheless, the sandwich hybridization methods combined with signal amplification strategy were often complicated, and required additional enzymes and other reagents, which limited their application in practical operation.

Herein, we developed a novel 1D PDA microtube waveguide platform which integrated with sandwich-structure design and condensing enrichment effect for miRNA-215 detection (as shown in Scheme 1). Two miRNA-complementary oligonucleotides were selected, which could bind to either two sides of the target miRNA-215. Single PDA microtube was modified with vinyl groups to interact with a thiol-modified capture probe (Probe 1) via click reaction. AuNRs were conjugated with another thiol-modified detection probe (Probe 2). When miRNA-215 was added to the system, it could be captured between two oligonucleotides which conjugated on PDA microtube and AuNR respectively, forming a sandwich-type complex and resulting in the out-coupled fluorescence of single PDA microtube quenching. By measuring the intensity variation of out-coupled tip emission, quantitative analysis of the target miRNA-215 could be achieved. Furthermore, due to the tethering of hydrophilic PDA microtube on the hydrophobic substrate and following condensing-enrichment effect, ultratrace miRNA sensing (the detection limit was as low as 8 pM) could be achieved without addition of DNA or enzyme reagents. The sensitive detection process could be completed in one step. Besides, the sandwich design and one step operation eliminated the defect of our previous work, and the developed PDA microtube waveguide platform exhibited outstanding stability and recyclability for miRNA detection. In addition, the early diagnosis and treatment of gastric cancer are of great concern [33]. Given that miRNA-215 plays an oncogene role in gastric carcinomas, and its over-expression in serum and gastric tissues of gastric cancer patients [34,35], the proposed biosensor was directly applied to discriminate the miRNA expression levels in clinical samples including gastric cancerous, paracancerous and normal tissues. It is anticipated that this proposed PDA microtube waveguide platform can be further applied to the detection of various biological analyte, which is meaningful for developing novel miRNAs quantification techniques for early clinical diagnosis of diseases.

2. Experimental

2.1. Reagents and instrumentation

All HPLC-purified miRNAs and DNA oligonucleotides used in this work were purchased from Shanghai Bio-Engineering Company (Shanghai, China), and the sequences of miRNA and DNA were shown in Table 1. Hybridization buffer (pH 8.0) (Tris-acetate/EDTA/Mg^{2+} buffer) contained 40 mM Tris-acetate, 2 mM ethylenediaminetetraacetic acid (EDTA), and 12.5 mM magnesium chloride. Milli-Q water purified system (18.2 MΩ cm) was used in all cases. 10, 12-Pentacosadiynoic acid (PCDA) were purchased from Tokyo Chemical Industry Co., Ltd. and purified to remove the polymerized part before use. All other solvents and reagents were of analytical grade and used as received. Gastric tissues were collected from Affiliated Provincial Hospital. Oligonucleotides were quantified by UV–vis absorption spectroscopy (the absorbance at 260 nm) which were recorded using a SHIMADZU UV-2550 PC spectrophotometer. Fluorescence spectra was measured by a JY-ihR 550 spectrophotometer. The Raman characterization was performed with a LABRAM-HR Confocal Laser Micro Raman Spectrometer with 514.5 nm radiation at room temperature. X-ray photoelectron spectroscopy (XPS) characterization was measured by a VG ESCALAB MK-II photoelectron spectrometer. Optical microscopy images were obtained with a BX-51 fluorescence microscope. The transmission electron microscopy (TEM) characterization was measured by a JEOL-2000 microscope (operated at 200 kV).

Table 1
Sequences of the used oligonucleotides (in 5′-3′ direction).

Name	Sequence
Probe 1	5′-SH-GGTCTGTTAATT-3′
Probe 2	5′-CATAGGTCATC-SH-3′
miRNA-215	5′-AUGACCUAUGAAUUAACAGAC-3′
single-base-mismatched miRNA-215	5′-AUGACCUAUGAAUUA AGAGAC-3′
three-base-mismatched miRNA-215	5′-AUGAGCUAUGGAUUAAGAGAC-3′
miRNA-21	5′-UAGCUUAUCAGACUGAUGUUGA-3′
miRNA-214	5′-UGCCUGUCUACACUUGCUGUGC-3′

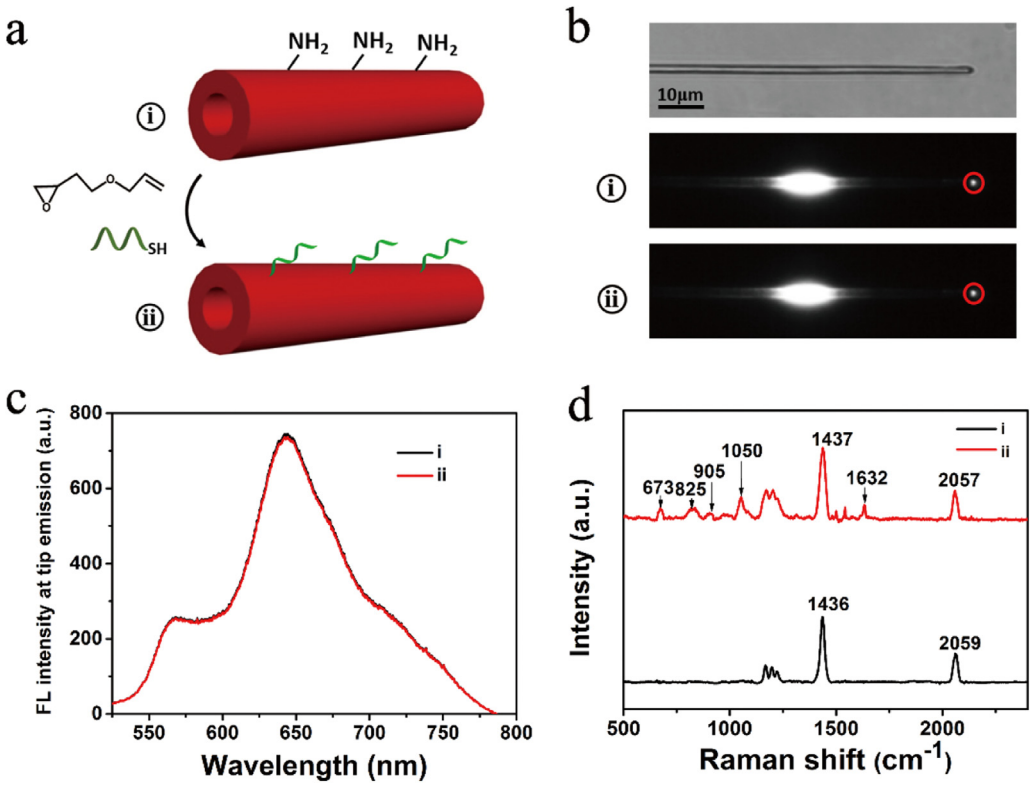

Fig. 1. (a) Synthesis of Probe 1 modified PDA microtube. (b) Optical waveguides of (i) single amine-functionalized PDA microtube and (ii) single Probe 1 modified PDA microtube. (c) Fluorescence intensity at tip emission of (i) amine-functionalized PDA microtube and (ii) Probe 1 modified PDA microtube. (d) Raman spectra of (i) amine-functionalized PDA microtube and (ii) Probe 1 modified PDA microtube.

2.2. The fabrication of Probe 1 conjugated PDA microtube and Probe 2 conjugated AuNR

Amine-functionalized PDA microtubes were prepared based on previously reported hierarchical self-assembly procedure [36]. Then 200 μL of allyl glycidyl ether (3 mmol) aqueous solution was injected into amine-functionalized PDA microtubes suspension solution to prepare vinyl-functionalized PDA microtubes [27]. Finally, thiol-modified DNA (Probe 1, 5′-SH-GGTCTGTTAATT-3′, 200 μL, 1 μmol) solution was added into the freshly prepared vinyl-functionalized PDA microtubes suspension. Thus, the Probe 1 conjugated PDA microtubes (DNA@PDA microtube) were prepared via click reaction, as described in Fig. 1a. The DNA modified Au nanorods were synthesized according to similar procedure as reported previously [37] (Fig. S2a). Another thiol-modified DNA (Probe 2, 5′- CATAGGTCATC-SH-3′, 10 μL, 100 μmol) solution was added dropwise to prepared AuNR solution. After incubation, the Probe 2 conjugated AuNRs (DNA@AuNR) were collected after three consecutive purification cycles involving centrifugation for 30 min at 9300 rpm and then dispersed in 10 mM PBS buffer. Both oligonucleotide conjugated PDA microtubes and AuNRs were stored at 4 °C.

2.3. Detection of target miRNA-215 in buffer and clinical samples

The glass substrate was coated with alkyl chain by octadecytrichlorosilane (OTS) as hydrophobic substrate before use. Then single DNA@PDA microtube was placed on hydrophobic substrate and adding a 10 μL droplet (containing the target miRNA-215 with various concentration and DNA@AuNR) to DNA@PDA microtube on hydrophobic substrate (Scheme 1). The optimum concentration of DNA@AuNR was illustrated in Fig. S3. From the data, at an optimal concentration of 0.5 nM, Au nanorods could effectively quench the fluorescence of microtube by formation of sandwich type complexes. After incubation at 15 °C for 2 h, PDA microtube was rinsed with PBS buffer for several times. A 532 nm excitation light was launched onto the body of the microtube and its out-coupled tip emission was characterized by single-tube PL imaging method, which was found to be dependent on the concentration of miRNA-215. We must note here that the intensity of excitation laser was 10 mW in all cases. To illustrate its selectivity, the platform was exposed to similarly sequenced miRNAs and non-complementary miRNAs. The reproducibility of the fluorescent response of the PDA microtube sensor system was also demonstrated by repeating detection process at miRNA-215 concentration of 1 nM for several times. To test anti-interference ability of the sensor, the prepared PDA microtubes were directly applied to detect miRNA-215 in complex biological environment, e.g. mixture containing 50% human serum in buffer. In the real sample detection, all the clinical gastric cancerous, paracancerous and normal tissues were pretreated with liquid nitrogen and followed by total miRNA extraction with RNA prep pure Tissue Kit. The detection experiments for the clinical samples were performed following the same procedure as mentioned above.

3. Results and discussion

3.1. Synthesis of DNA@PDA microtube and DNA@AuNR

To improve the stability and recyclability of the PDA microtube waveguide platform, the co-hybridization design of the target miRNA-215 with DNA@PDA microtube and DNA@AuNR was employed. The fabrication of the DNA@PDA microtube was illustrated in Fig. 1a. Amine-functionalized PDA microtubes were prepared by a hierarchical self-assembly procedure as reported previously [36]. After incubating with aqueous solution of allylglycidyl ether for 2 h, two new bands (1130 cm^{-1} for C-O-C stretching vibration and 923 cm^{-1} for C=CH stretching vibration) emerged in FT-IR spectra (Fig. S1b), indicating successful modification with the vinyl groups on the surface of PDA microtube. Then oligonucleotide conjugated PDA microtube could be fabricated via “thiol-ene” based click reaction. After incubating with aqueous solution of Probe 1 upon UV irradiation for 6 h, qualitative analysis of PDA microtube were performed by optical waveguide and Raman spectra characterization. The waveguide properties of single PDA microtube could be characterized by single-tube PL imaging method (Fig. 1b and c). A 532 nm excitation light was launched towards

the microtube first. Then a notable spot of bright PL could be observed at the tip of the microtube, while comparatively equal emission emanated from the body of PDA microtube after modification with Probe 1. The propagation loss of Probe 1 conjugated PDA microtube was estimated to be about 0.20 dB μm^{-1}, similar to that of pure PDA microtube (0.18 dB μm^{-1}) before reaction. These results indicated that the conjugation with Probe 1 did not significantly affect the waveguide properties of PDA microtube, and the dominant optical loss mechanism should be mainly ascribed to the reabsorption and light scattering effect [36]. Raman spectroscopy was also used to characterize the properties of PDA microtube after reaction. As shown in Fig. 1d, before click reaction, Raman vibrational bands at 1436 and 2059 cm^{-1} were ascribed to the to the C=C and C≡C stretching vibrations of PDA backbone, respectively. After modification with Probe 1, new bands emerged at 673, 825, 905, 1050, 1632 cm^{-1}, which should be attributed to the ring stretching mode in guanine, ring breathing mode in cytosine, CN bond stretching in guanine, symmetric stretching of phosphate backbone, and C=O bond stretching in thymine, respectively. These results demonstrated the successful anchoring of Probe 1 on the surface of PDA microtube. The density of the modified Probe 1 on the surface of PDA microtube was calculated to be about 20 fmol•μm^{-2}, by quantitatively analyzing the relative absorbance change at 260 nm of the Probe 1 solution before and after reaction with PDA microtube.

The Probe 2 conjugated Au nanorods were successfully prepared following similar procedure reported previously [37]. The electrophoresis analysis results demonstrated that DNA@AuNR run slower than unconjugated Probe 2 (Fig. S2b). Characterization of UV absorption also proved successful preparation of DNA@AuNR. After conjugation with Probe 2, the longitudinal peak of AuNR blue-shifted from 664 nm to 645 nm (Fig. S2d). The amount of the conjugated oligonucleotides to each Au nanorod was estimated to be about 800. The absorption band of DNA@AuNR overlaps with the out-coupled fluorescence spectra of PDA microtube. Therefore, it is anticipated that the formation of a sandwich structure, as a result of the co-hybridization of target miRNA with DNA@PDA microtube and DNA@AuNR, might bring AuNR close to the surface of microtube, resulting in out-coupled fluorescence of PDA microtube extinction.

3.2. Sensitive and selective detection of miRNA 215 in buffer samples

As reported previously [38], the analytes would be enriched and anchored on the hydrophilic surface of PDA microtube when PDA microtube was placed on the hydrophobic substrate, which should be ascribed to the difference of surface free energy between the hydrophilic surface of PDA microtube and the hydrophobic substrate. The analyte droplet would concentrate to a small area after solvent evaporation. It is expected that the condensing-enrichment approach could fulfill ultratrace miRNA sensing. As shown in Fig. 2a, a drop (10 μL) of buffer solution containing DNA@AuNR (0.5 nM) and the target miRNA-215 (100 nM) was added on the surface of PDA microtube waveguide platform, and then the platform was dried at 15 °C and 40% relative humidity. In the initial stage of the reaction, the drop let would not spread out and concentrated in a small area. As the reaction proceeded, the volume of droplet decreased and the concentration of the reactant increased remarkably. The reactant enriched on the surface of microtube and the signal would be amplified. The decrease of the droplet volume resulted in more successful collision of analytes, therefore, the sensitivity of the detection platform could be significantly improved. Changes in the out-coupled emission intensity at the tip of PDA microtube with increased reaction time were illustrated in Fig. 2b. The fluorescence of PDA microtube was diminished because Au nanorods could serve as quencher to diminish the fluorescence of PDA microtube after sandwich structure forming process (AuNR was very close to the surface of PDA microtube to trigger FRET effect). The relative variation of tip emission intensity at 640 nm was reached about 30% in 20 min. It was reasonable to determine the response time of the designed platform based on the chronological development of the relative change in tip emission at 640 nm (Fig. 2c). The signal variation gained its maximum over 120 min, which was defined as optimum reaction time. However, when the reaction was carried out in 200 μL buffer solution, the signal at 100 nM only reached to 120 (Fig. S4a). At the same concentration, the signal could reach to 710 with condensing enrichment effect (Fig. 2b). It is further proved that the condensing enrichment effect could effectively amplify the signal without additional enzyme reagents. Then the proposed biosensor was used to detect miRNA-215 with various concentrations and the waveguide properties of single PDA microtube were characterized in detail (Fig. 3a). Obvious quenching of the out-coupled tip emission could be easily observed even at very low concentration of the target miRNA-215 (100 pM). The out-coupled tip emission intensity monotonically decreased with logarithm of target miRNA-215 concentration. And completely emission change was observed when the concentration of target miRNA-215 increased to 100 nM. As illustrated in Fig. 3b, the fluorescence intensity decreased exponentially with the concentration of target miRNA-215, which should be mainly ascribed to condensing enrichment effect. The detection limit of the PDA microtube waveguide platform (3σ/slope) was calculated to be 8 pM, comparable to the typical levels of miRNA in serum [39]. Compared with reaction in 200 μL buffer solution (Fig. S4b, the LOD was 1.6 nM), at least a two order increase in the sensitivity could be obtained with condensing enrichment effect. Besides, the large aspect ratio of PDA microtubes could facilitate the adsorption and reaction of reactants through the wall. Reactions happened at any point among the excitation position and the emission out-coupling position could also lead to a sensitive signal change. Further, the reproducibility of PDA microtube waveguide platform was demonstrated by relative standard deviation (RSD). As shown in Fig. S5, six replicate detection process of miRNA-215 at 1 nM were investigated, and the corresponding RSD values of the relative change in tip emission was calculated to be 3.6%, indicating acceptable reproducibility of the proposed method. Furthermore, the proposed method was compared with other signal amplification methods for miRNA or DNA detection (Table 2). The corresponding results shows that, compared to other methods, the PDA microtube platform could easily achieved highly sensitive detection of miRNA in one step without additional DNA or enzyme reagents. These results indicated that the sandwich type biosensor could be applied to accurate quantitation of target miRNA-215 in aqueous solution.

The feasible detection of target miRNA-215 in complex conditions is crucial for the practical application of PDA microtube waveguide platform. It is essential to assess the analytical selectivity and specificity against possible interferences. Four kinds of miRNAs with high sequence similarity (including single-base mismatched miRNA-215, three-base mismatched miRNA-215 and two non-complementary miRNAs, miRNA-214, miRNA-21) were selected to investigate the selectivity of PDA microtube waveguide platform. As shown in Fig. S6, no obvious fluorescence variation could be detected upon addition of other miRNAs at concentration as high as 10 nM. Even miRNA-215 with only one single base mutation in the middle also could be clearly distinguished. However, upon addition of only 0.1 nM miRNA-215, significant change in tip emission was observed. Take the case of 1 nM for example, fluorescence variation caused by miRNA-215 displayed more than three times larger than that caused by single-base mismatched miRNA-215 (Fig. 4a). These results well confirmed that the designed PDA microtube waveguide platform could act as highly selective probe for miRNA-215 detection. Another essential requirement was negligible interference from other miRNAs with high sequence similarity. As shown in Fig. 4b, upon adding the mixture of other four miRNAs (each 0.5 nM), only weak fluorescence variation (35%) cloud be detected. However, upon addition of 0.1 nM miRNA-215, remarkable change in tip emission could be detected, indicating minor interference from other miRNAs. All these results suggested that the designed PDA microtube waveguide platform could detect miRNA-215 selectively, even in the presence of other miRNAs with high sequence similarity, which

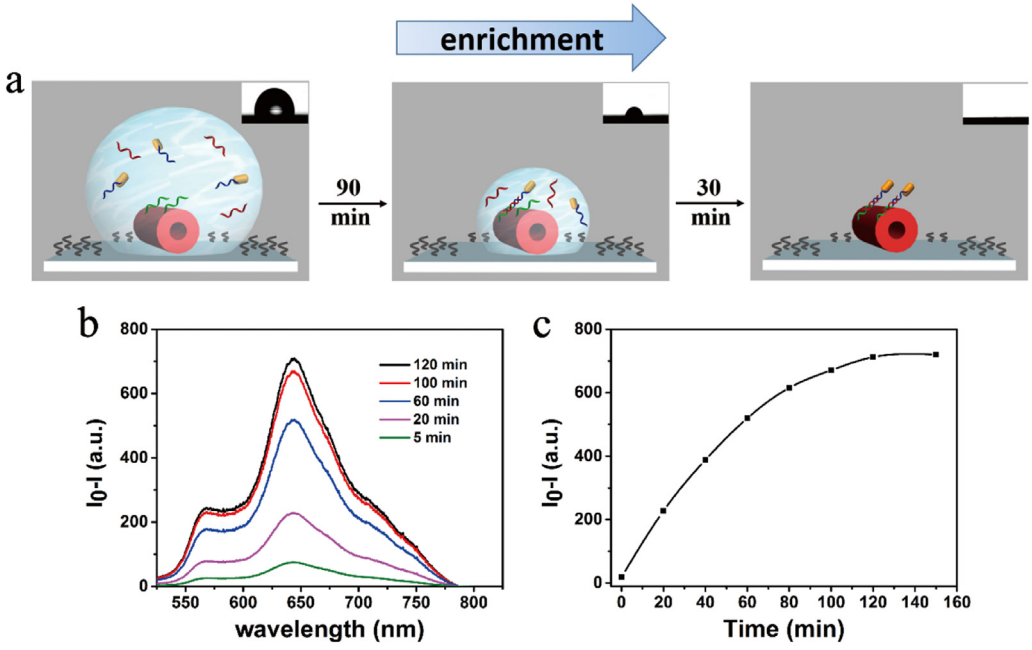

Fig. 2. (a) Schematic illustration of the condensing enrichment effect, a hydrophilic DNA@PDA microtube placed on a hydrophobic substrate and a droplet contained miRNA-215 and DNA@AuNR was added on the DNA@PDA microtube. (b) Changes in the out-coupled emission at the tip of PDA microtube with increased reaction time upon addition of 100 nM miRNA-215. I_0 and I represent the tip emission intensity of PDA microtube before and after reaction with miRNA-215, respectively. (c) Time dependent relative change in tip emission at 640 nm of the microtube upon addition of 100 nM miRNA-215.

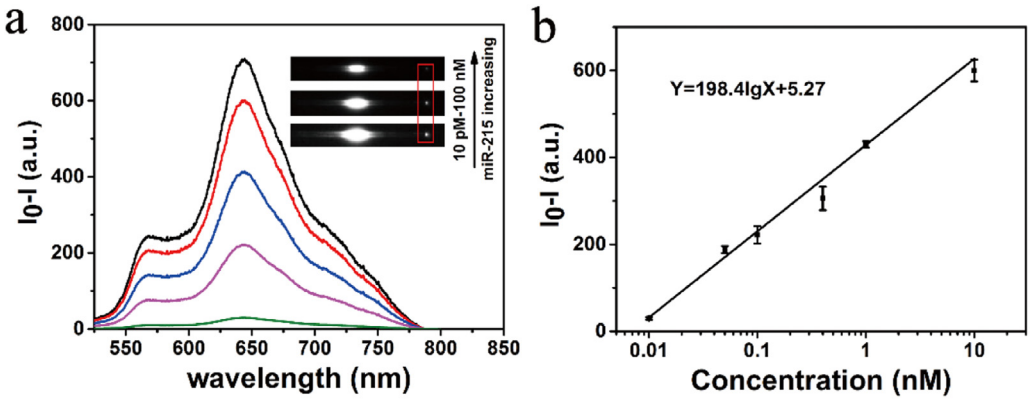

Fig. 3. (a) Changes in the out-coupled emission at the tip of PDA microtube with increased concentration of miRNA-215. (b) Plot of variation of out-coupled tip emission intensity at 640 nm upon gradual addition of miRNA-215 (ranged from 0.01 to 10 nM).

Table 2
Comparison of different methods for miRNA/DNA detection.

Detection methods	Target	Signal amplification strategy	LOD	Ref
Electrochemical	miRNA-221	Supersandwich structure	0.6 pM	[47]
Colorimetry	miRNA-224	TMB/H_2O_2 enzymatic substrate	7.5 pM	[48]
Colorimetry	HCV-1 DNA	Rolling circle amplification	10 pM	[49]
Fluorescence	miRNA-21	Exo I- assisted	500 pM	[50]
Fluorescence	miRNA-21	Catalyzed hairpin assembly	3.5 pM	[51]
Fluorescence	miRNA-215	Condensing enrichment effect	8 pM	Present work

further supported its feasibility of practical application in complex environment.

It is a remarkable fact that our previous work with directly toehold strand displacement design has the defects of irreversibility and weak storage stability, which limit its practical applications. Therefore, it was strongly hoped to establish a recyclable platform with acceptable storage stability. For the validation of recyclability, after the first-round reaction, the sandwich type PDA microtube platform was heated to 50 °C and rinsed with 0.1 M PBS buffer thoroughly, which resulted in the broken of the sandwich structure. And the revival of tip emission intensity could be observed due to the removal of AuNR from the surface of PDA microtube. As shown in Fig. 5a, the fluorescence of the PDA microtube and tip emission could both returned to the original value, almost the same as the value before miRNA-215 detection. XPS spectrum was also used to verify this process. When sandwich structure formed, Au 4f core level region contained two peaks (84.5 and 88.1 eV, respectively) could be observed, indicated the anchoring of Au nanorods on the microtube. While, after regeneration process, these peaks disappeared in spectrum (Fig. S7). Two more regeneration and reuse cycles exhibited similar tip emission variation, clearly indicating that the proposed PDA microtube waveguide platform could serve as a reusable probe for miRNA-215 detection (Fig. 5b). The storage stability is also a key factor of the proposed biosensor in its application and development. Five as-prepared DNA@PDA microtubes were stored at 4 °C and every one of them was taken out for detection experiments at different storage times (0, 5, 10, 15 and 20 days). Compared to the PDA microtube waveguide platform with directly toehold strand displacement design (AuNR@PDA microtube), the storage stability of PDA microtube waveguide platform with sandwich co-hybridization design (DNA@PDA microtube) is significantly enhanced. As shown in Fig. 5c,

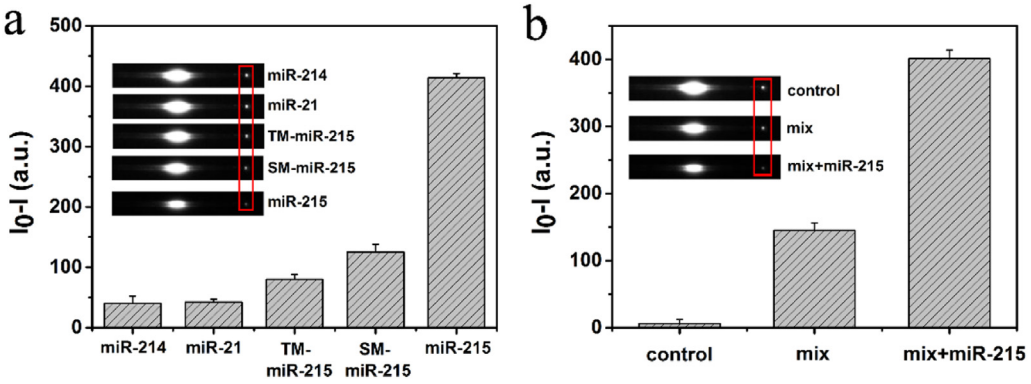

Fig. 4. (a) Selectivity investigation of the proposed method for single-base mismatched miRNA-215, three-base mismatched miRNA-215 and miRNA-214, miRNA-21, miRNA-215 with the same concentration (1 nM). (b) The fluorescence change in tip emission at 640 nm with a mixture of other RNAs (mix: single-base mismatched miRNA-215, three-base mismatched miRNA-215, miRNA-21, miRNA-214, each 0.5 nM) before and after addition of miRNA-215 (0.1 nM) to above mixture solution.

no significant reaction efficiency variation could be detected after 5 days of storage, and the proposed biosensor reserved about 75% of its original response when the storage time was extended to 20 days. Compared to the superior stability of DNA@PDA microtubes, the reaction efficiency of AuNR@PDA decreased significantly with the increased storage time. The instability of AuNR@PDA microtube is attributed to the fact that the Au nanorods are not stable in buffers at high salt concentration. In addition, owing to strong adhesion of Au nanorod on the surface of PDA microtube, the fluorescence of PDA microtube would substantially be quenched completely after long-term storage. Sandwich type design could eliminate this defect of Au nanorods, because DNA@PDA microtubes was enough stable in buffer. The results indicated that the proposed PDA microtube waveguide platform had acceptable storage stability. All these results suggested that sandwich co-hybridization design could improve both the stability and the recyclability of PDA microtube waveguide platform.

The environmental stability of biosensors in complex matrix, e.g. in human serum, is of much importance for biomedical applications. Therefore, the analytical performance of the proposed PDA microtube sensor in the buffer mixture solution containing 50% human serum was evaluated compared to that in Tris buffer. As shown in Fig. 5d, signal variation of PDA microtube gradually increased with the increase of miRNA-215 concentration. The signal variation in serum slightly decreased relative to that in buffer, which should be attributed to the interference from high-molecular-weight DNAs, plasma protein, and other substance in serum. These results further supported the practicability of proposed PDA microtube waveguide platform in complex biological environment.

3.3. Detection of miRNA-215 in clinical samples

At present, it has been found that the expression of miRNA-215 is down-regulated in esophageal cancer, renal carcinoma, colon cancer and other tumor tissues, which plays the role of tumor suppressor gene in the occurrence and development of these cancers [40–42]. Unlike other solid tumors, the expression level of miRNA-215 in gastric cancer is significantly increased [43], which can play the role of oncogenes and promote ability of cell proliferation and invasion of tumor cells. Considering of the undeniable diagnostic value of miRNA-215 expression level in gastric cancer tissues, the usefulness of the developed detection method was evaluated for the determination and quantification of miRNA-215 extracted from different tumor sites in gastric cancer

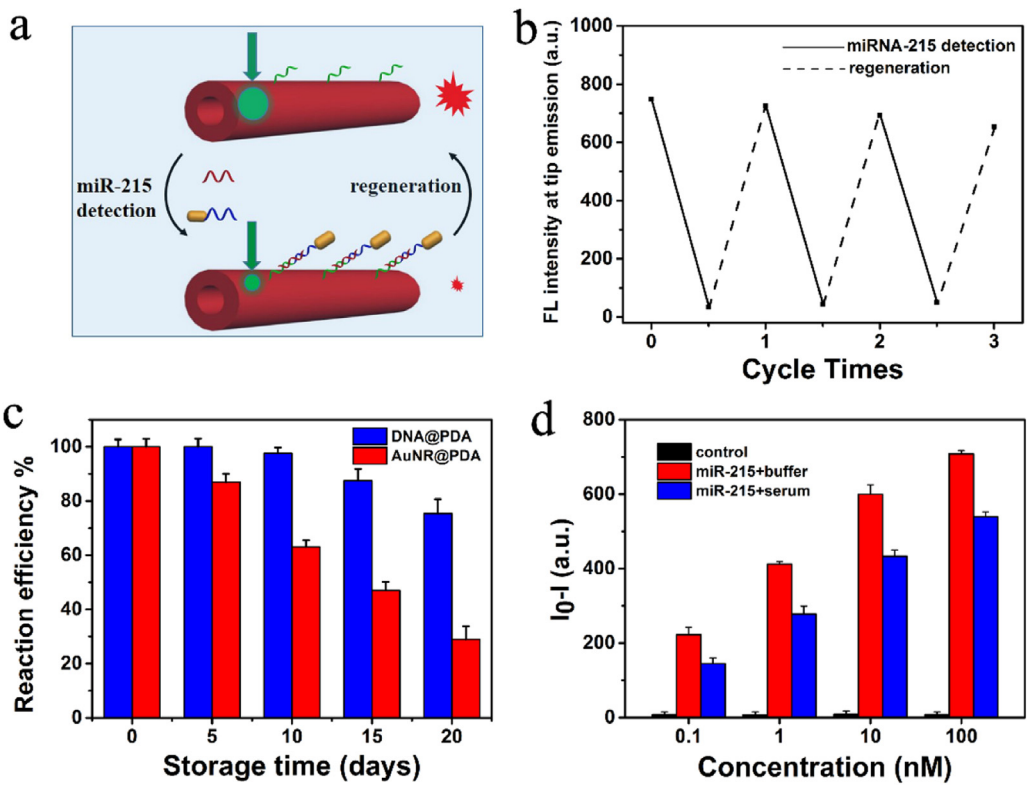

Fig. 5. (a) Schematic representation of reversible optical response of PDA microtube waveguide platform for miRNA detection. (b) Fluorescence intensity change in tip emission (at 640 nm) of PDA microtube during miRNA-215 detection and regeneration process. (c) The storage stability of the proposed DNA@PDA biosensor and AuNR@PDA biosensor. (d) The fluorescence variation of tip emission for single PDA microtube after reaction in control solution (without miRNA-215), in Tris buffer and in the buffer mixture solution containing 50% diluted human serum.

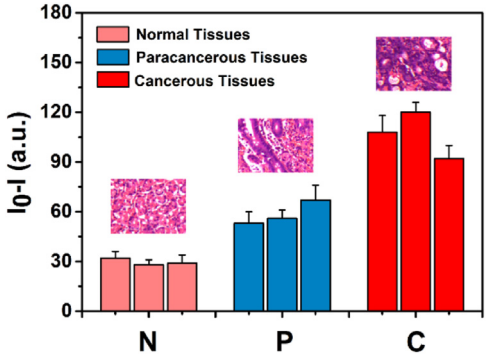

Fig. 6. Detection of mature miRNA-215 extracted from gastric cancerous (C), paracancerous (P) and normal (N) tissues and their pathological characterization.

tissues. In addition, the miRNA-215 detection in different tumor sites is helpful for resection of tumor tissues during operation. In this study, the miRNA-215 expression levels in gastric cancerous, paracancerous and normal tissues were detected by the proposed PDA microtube waveguide platform. All clinical samples were pretreated with liquid nitrogen and followed by total miRNA extraction with RNA prep pure Tissue Kit. As shown in Fig. 6, no obvious fluorescence variation cloud be detected after reaction with samples extracted from normal tissues. And the signal of the sample extracted from gastric cancerous tissues was about 2-fold larger than those of the sample extracted from paracancerous tissues. Therefore, the proposed PDA microtube biosensor allows the reliable detection miRNA-215 expression levels extracted from tissues. The results were consistent with previous reports, which validated the practicability of our proposed methods [34,35,44–46]. Considering that the tumor tissues and normal tissues are intertwined, it is necessary to identification the expression levels of miRNA-215 in adjacent parts, which is helpful for resection of tumor location. It is suggested that miRNA-215 is related to the formation of gastric cancer, so it has potential as a marker for the diagnosis of gastric cancer. Hence this miRNAs detection platform possesses potentials to be a versatile strategy for tumor molecular diagnosis technologies, and high precision of miRNA expression levels can be achieved by increasing sample dose and multidraw of tumor tissue.

4. Conclusions

In summary, a novel highly sensitive and selective PDA microtube waveguide platform with enhanced recyclability and acceptable storage stability has been developed for miRNA-215 determination. The combination of sandwich hybridization with condensing enrichment effect realized highly sensitive miRNA detection in one step. The sandwich structure formed as a result of co-hybridization of target miRNA. The reaction of oligonucleotides allowed the AuNR to be anchored on the surface of PDA microtube, which was sufficiently close to trigger FRET effect. The intensity of the out-coupled tip emission varied with miRNA-215 concentration, allowing for quantitative determination of target miRNA-215. More importantly, our methods have been tested in real clinical samples and achieved satisfactory results for discrimination of miRNA-215 expression levels in gastric cancerous, paracancerous and normal tissues. With reliance on the instinctive properties proposed above, the PDA microtube waveguide platform possesses potentials to be a versatile strategy for tumor molecular diagnosis technologies, and could be extended to other proteins or new biomarkers for disease diagnosis and clinical fundamental research.

Acknowledgements

Financial support from the National Natural Science Foundation of China (21574120, 21774115), the Basic Research Fund for the Central Universities (WK2060200025), the Science and Technological Fund of Anhui Province for Outstanding Youth (1608085J01).

Appendix A. Supplementary material

Supplementary data associated with this article can be found in the online version at http://dx.doi.org/10.1016/j.talanta.2018.05.049.

References

[1] A.D. Castañeda, N.J. Brenes, A. Kondajji, R.M. Crooks, Detection of microRNA by Electrocatalytic Amplification: a General Approach for Single-Particle Biosensing, J. Am. Chem. Soc. 139 (2017) 7657–7664.
[2] F. Causa, A. Aliberti, A.M. Cusano, E. Battista, P.A. Netti, Supramolecular spectrally encoded microgels with double strand probes for absolute and direct miRNA fluorescence detection at high sensitivity, J. Am. Chem. Soc. 137 (2015) 1758–1761.
[3] L. Liang, F. Lan, X. Yin, S. Ge, J. Yu, M. Yan, Metal-enhanced fluorescence/visual bimodal platform for multiplexed ultrasensitive detection of microRNA with reusable paper analytical devices, Biosens. Bioelectron. 95 (2017) 181–188.
[4] M.J. Lodes, M. Caraballo, D. Suciu, S. Munro, A. Kumar, B. Anderson, Detection of cancer with serum miRNAs on an oligonucleotide microarray, PloS One 4 (2009) e6229.
[5] G.A. Calin, C.D. Dumitru, M. Shimizu, R. Bichi, S. Zupo, E. Noch, H. Aldler, S. Rattan, M. Keating, K. Rai, Frequent deletions and down-regulation of micro-RNA genes miR15 and miR16 at 13q14 in chronic lymphocytic leukemia, Proc. Natl. Acad. Sci. USA 99 (2002) 15524–15529.
[6] A. Zampetaki, S. Kiechl, I. Drozdov, P. Willeit, U. Mayr, M. Prokopi, A. Mayr, S. Weger, F. Oberhollenzer, E. Bonora, Plasma MicroRNA profiling reveals loss of endothelial MiR-126 and other MicroRNAs in type 2 DiabetesNovelty and significance, Circ. Res. 107 (2010) 810–817.
[7] J. Zhu, T. Chen, L. Yang, Z. Li, M.M. Wong, X. Zheng, X. Pan, L. Zhang, H. Yan, Regulation of microRNA-155 in atherosclerotic inflammatory responses by targeting MAP3K10, PloS One 7 (2012) e46551.
[8] S. Volinia, M. Galasso, S. Costinean, L. Tagliavini, G. Gamberoni, A. Drusco, J. Marchesini, N. Mascellani, M.E. Sana, R.A. Jarour, Programming of miRNA networks in cancer and leukemia, Genome Res. 20 (2010) 589–599.
[9] K. McDaniel, L. Herrera, T. Zhou, H. Francis, Y. Han, P. Levine, E. Lin, S. Glaser, G. Alpini, F. Meng, The functional role of microRNAs in alcoholic liver injury, J. Cell. Mol. Med. 18 (2014) 197–207.
[10] P. Trionfini, A. Benigni, G. Remuzzi, MicroRNAs in kidney physiology and disease, Nat. Rev. Nephrol. 11 (2015) 23–33.
[11] N. Yanaihara, N. Caplen, E. Bowman, M. Seike, K. Kumamoto, M. Yi, R.M. Stephens, A. Okamoto, J. Yokota, T. Tanaka, Unique microRNA molecular profiles in lung cancer diagnosis and prognosis, Cancer Cell 9 (2006) 189–198.
[12] Y. Chen, J.A. Gelfond, L.M. McManus, P.K. Shireman, Reproducibility of quantitative RT-PCR array in miRNA expression profiling and comparison with microarray analysis, BMC Genom. 10 (2009) 407–416.
[13] D. Zubakov, A.W. Boersma, Y. Choi, P.F. van Kuijk, E.A. Wiemer, M. Kayser, MicroRNA markers for forensic body fluid identification obtained from microarray screening and quantitative RT-PCR confirmation, Int. J. Leg. Med. 124 (2010) 217–226.
[14] S. Sharbati-Tehrani, B. Kutz-Lohroff, R. Bergbauer, J. Scholven, R. Einspanier, miR-Q: a novel quantitative RT-PCR approach for the expression profiling of small RNA molecules such as miRNAs in a complex sample, BMC Mol. Biol. 9 (2008) 34–46.
[15] Y. Ren, H. Deng, W. Shen, Z. Gao, A highly sensitive and selective electrochemical biosensor for direct detection of microRNAs in serum, Anal. Chem. 85 (2013) 4784–4789.
[16] M. Labib, N. Khan, S.M. Ghobadloo, J. Cheng, J.P. Pezacki, M.V. Berezovski, Three-mode electrochemical sensing of ultralow microRNA levels, J. Am. Chem. Soc. 135 (2013) 3027–3038.
[17] A. Válóczi, C. Hornyik, N. Varga, J. Burgyán, S. Kauppinen, Z. Havelda, Sensitive and specific detection of microRNAs by northern blot analysis using LNA-modified oligonucleotide probes, Nucleic Acids Res. 32 (2004) (e175-e175).
[18] G.S. Pall, A.J. Hamilton, Improved northern blot method for enhanced detection of small RNA, Nat. Protoc. 3 (2008) 1077–1084.
[19] P.T. Nelson, D.A. Baldwin, L.M. Scearce, J.C. Oberholtzer, J.W. Tobias, Z. Mourelatos, Microarray-based, high-throughput gene expression profiling of microRNAs, Nat. Methods 1 (2004) 155–161.
[20] J.M. Thomson, J. Parker, C.M. Perou, S.M. Hammond, A custom microarray platform for analysis of microRNA gene expression, Nat. Methods 1 (2004) 47–53.
[21] B.-C. Yin, Y.-Q. Liu, B.-C. Ye, One-step, multiplexed fluorescence detection of microRNAs based on duplex-specific nuclease signal amplification, J. Am. Chem. Soc. 134 (2012) 5064–5067.
[22] S.W. Yang, T. Vosch, Rapid detection of microRNA by a silver nanocluster DNA probe, Anal. Chem. 83 (2011) 6935–6939.
[23] A.N. Silahtaroglu, D. Nolting, L. Dyrskjøt, E. Berezikov, M. Møller, N. Tommerup, S. Kauppinen, Detection of microRNAs in frozen tissue sections by fluorescence in situ hybridization using locked nucleic acid probes and tyramide signal amplification, Nat. Protoc. 2 (2007) 2520–2528.
[24] H.T. Hoang, T. Lee, B.-S. Kim, K.-C. Han, D.-R. Ahn, An immunoassay utilizing the

DNA-coated polydiacetylene micelles as a signal generator, Bioorg. Med. Chem. Lett. 23 (2013) 2675–2678.
[25] F. Degliangeli, P. Kshirsagar, V. Brunetti, P.P. Pompa, R. Fiammengo, Absolute and direct microRNA quantification using DNA–gold nanoparticle probes, J. Am. Chem. Soc. 136 (2014) 2264–2267.
[26] R.-Q. Liang, W. Li, Y. Li, C.-y. Tan, J.-X. Li, Y.-X. Jin, K.-C. Ruan, An oligonucleotide microarray for microRNA expression analysis based on labeling RNA with quantum dot and nanogold probe, Nucleic Acids Res. 33 (2005) (e17-e17).
[27] Y. Zhu, D. Qiu, G. Yang, M. Wang, Q. Zhang, P. Wang, H. Ming, D. Zhang, Y. Yu, G. Zou, Selective and sensitive detection of MiRNA-21 based on gold-nanorod functionalized polydiacetylene microtube waveguide, Biosens. Bioelectron. 85 (2016) 198–204.
[28] Y. Jiang, N. Liu, W. Guo, F. Xia, L. Jiang, Highly-efficient gating of solid-state nanochannels by DNA supersandwich structure containing ATP aptamers: a nanofluidic IMPLICATION logic device, J. Am. Chem. Soc. 134 (2012) 15395–15401.
[29] F. Xia, R.J. White, X. Zuo, A. Patterson, Y. Xiao, D. Kang, X. Gong, K.W. Plaxco, A.J. Heeger, An electrochemical supersandwich assay for sensitive and selective DNA detection in complex matrices, J. Am. Chem. Soc. 132 (2010) 14346–14348.
[30] N. Zhang, D.H. Appella, Colorimetric detection of anthrax DNA with a peptide nucleic acid sandwich-hybridization assay, J. Am. Chem. Soc. 129 (2007) 8424–8425.
[31] X. Gao, L.-P. Xu, T. Wu, Y. Wen, X. Ma, X. Zhang, An enzyme-amplified lateral flow strip biosensor for visual detection of microRNA-224, Talanta 146 (2016) 648–654.
[32] A. Qureshi, Y. Gurbuz, J.H. Niazi, Capacitive aptamer–antibody based sandwich assay for the detection of VEGF cancer biomarker in serum, Sens. Actuators B 209 (2015) 645–651.
[33] A. Jemal, F. Bray, M.M. Center, J. Ferlay, E. Ward, D. Forman, Global cancer statistics, CA: Cancer J. Clin. 61 (2) (2011) 69–90.
[34] Z. Jin, F. Selaru, Y. Cheng, T. Kan, R. Agarwal, Y. Mori, A. Olaru, J. Yang, S. David, J. Hamilton, MicroRNA-192 and-215 are upregulated in human gastric cancer in vivo and suppress ALCAM expression in vitro, Oncogene 30 (13) (2011) 1577.
[35] D.P. Bartel, MicroRNAs: target recognition and regulatory functions, Cell 136 (2) (2009) 215–233.
[36] W. Hu, Y. Chen, H. Jiang, J. Li, G. Zou, Q. Zhang, D. Zhang, P. Wang, H. Ming, Optical waveguide based on a polarized polydiacetylene microtube, Adv. Mater. 26 (2014) 3136–3141.
[37] I.C. Pekcevik, L.C. Poon, M.C. Wang, B.D. Gates, Tunable loading of single-stranded DNA on gold nanorods through the displacement of polyvinylpyrrolidone, Anal. Chem. 85 (2013) 9960–9967.
[38] L.P. Xu, Y. Chen, G. Yang, W. Shi, B. Dai, G. Li, Y. Cao, Y. Wen, X. Zhang, S. Wang, Ultratrace DNA detection based on the condensing-enrichment effect of superwettable microchips, Adv. Mater. 27 (2015) 6878–6884.
[39] R. Wilson, A.R. Cossins, D.G. Spiller, Encoded microcarriers for high-throughput multiplexed detection, Angew. Chem. Int. Ed. 45 (2006) 6104–6117.
[40] B. Song, Y. Wang, M.A. Titmus, G. Botchkina, A. Formentini, M. Kornmann, J. Ju, Molecular mechanism of chemoresistance by miR-215 in osteosarcoma and colon cancer cells, Mol. Cancer 9 (2010) 96.
[41] S.A. Georges, M.C. Biery, S.-y. Kim, J.M. Schelter, J. Guo, A.N. Chang, A.L. Jackson, M.O. Carleton, P.S. Linsley, M.A. Cleary, Coordinated regulation of cell cycle transcripts by p53-Inducible microRNAs, miR-192 and miR-215, Cancer Res. 68 (2008) 10105–10112.
[42] H.W. Khella, M. Bakhet, G. Allo, M.A. Jewett, A.H. Girgis, A. Latif, H. Girgis, I. Von Both, G.A. Bjarnason, G.M. Yousef, miR-192, miR-194 and miR-215: a convergent microRNA network suppressing tumor progression in renal cell carcinoma, Carcinogenesis 34 (2013) 2231–2239.
[43] Y. Deng, Z. Huang, Y. Xu, J. Jin, W. Zhuo, C. Zhang, X. Zhang, M. Shen, X. Yan, L. Wang, MiR-215 modulates gastric cancer cell proliferation by targeting RB1, Cancer Lett. 342 (2014) 27–35.
[44] J.H. Song, S.J. Meltzer, MicroRNAs in pathogenesis, diagnosis, and treatment of gastroesophageal cancers, Gastroenterology 143 (1) (2012) 35–47 (e2).
[45] Y. Xu, Y. Fan, MiR-215/192 participates in gastric cancer progression, Clin. Transl. Oncol. 17 (1) (2015) 34–40.
[46] Y. Deng, Z. Huang, Y. Xu, J. Jin, W. Zhuo, C. Zhang, X. Zhang, M. Shen, X. Yan, L. Wang, MiR-215 modulates gastric cancer cell proliferation by targeting RB1, Cancer Lett. 342 (1) (2014) 27–35.
[47] H. Zhang, Q. Wang, X. Yang, K. Wang, Q. Li, Z. Li, L. Gao, W. Nie, Y. Zheng, An isothermal electrochemical biosensor for the sensitive detection of microRNA based on a catalytic hairpin assembly and supersandwich amplification, Analyst 142 (2017) 389–396.
[48] X. Gao, L.-P. Xu, T. Wu, Y. Wen, X. Ma, X. Zhang, An enzyme-amplified lateral flow strip biosensor for visual detection of microRNA-224, Talanta 146 (2016) 648–654.
[49] M. Liu, C.Y. Hui, Q. Zhang, J. Gu, B. Kannan, S. Jahanshahi-Anbuhi, C.D. Filipe, J.D. Brennan, Y. Li, Target-induced and equipment-free DNA amplification with a simple paper device, Angew. Chem. 128 (2016) 2759–2763.
[50] C. Ma, H. Liu, K. Wu, M. Chen, L. Zheng, J. Wang, An exonuclease I-based quencher-free fluorescent method using DNA hairpin probes for rapid detection of MicroRNA, Sensors 17 (2017) 760.
[51] C. Liu, S. Lv, H. Gong, C. Chen, X. Chen, C. Cai, 2-aminopurine probe in combination with catalyzed hairpin assembly signal amplification for simple and sensitive detection of microRNA, Talanta 174 (2017) 336–340.